Extracting Sequential Features from Dynamic Connectivity Network with rs-fMRI Data for AD Classification

Kai Lin[1], Biao Jie[1](✉), Peng Dong[1], Xintao Ding[1], Weixin Bian[1], and Mingxia Liu[2]

[1] School of Computer and Information, Anhui Normal University, Wuhu 241003, Anhui, China
jbiao@ahnu.edu.cn

[2] Department of Radiology and BRIC, University of North Carolina at Chapel Hill, Chapel Hill, NC 27599, USA

Abstract. Dynamic functional connectivity (dFC) networks based on resting-state functional magnetic resonance imaging (rs-fMRI) can help us understand the function of brain better, and have been applied to brain disease identification, such as Alzheimer's disease (AD) and its early stages (*i.e.*, mild cognitive impairment, MCI). Deep learning (*e.g.*, convolutional neural network, CNN) methods have been recently applied to dynamic FC network analysis, and achieve good performance compared to traditional machine learning methods. Existing studies usually ignore sequence information of temporal features from dynamic FC networks. To this end, in this paper, we propose a recurrent neural network-based learning framework to extract sequential features from dynamic FC networks with rs-fMRI data for brain disease classification. Experimental results on 174 subjects with baseline resting-state functional MRI (rs-fMRI) data from ADNI demonstrate the effectiveness of our proposed method in binary and multi-category classification tasks.

1 Introduction

Alzheimer's disease (AD) is a common neurodegenerative disease in the elderly and the most common cause of dementia, characterized by progressive cognitive impairment [1]. Its prodromal stage, called mild cognitive impairment (MCI), has received widespread attention because of its high possibility of developing into AD [2–4]. The accurate progression prediction of AD-related disorders is of great significance for early treatment and delaying the deterioration of the disease. Resting-state functional magnetic resonance imaging (rs-fMRI) provides a non-invasive solution to objectively measure the activity of human brain neurons [5]. Functional connectivity (FC) networks based on rs-fMRI can characterize neural interactions between brain regions and have been applied to various AD-related brain disease diagnosis [6–10].

Existing research on FC networks is generally based on temporal correlation between distributed brain regions, implicitly assuming that functional connectivity of the human brain is static during the entire fMRI recording period [11].

C. Lian et al. (Eds.): MLMI 2021, LNCS 12966, pp. 664–673, 2021.
https://doi.org/10.1007/978-3-030-87589-3_68

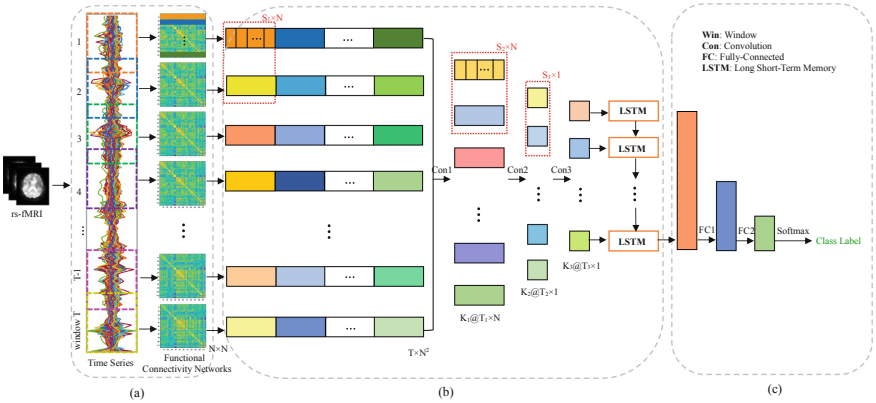

Fig. 1. Illustration of the proposed RNN-based learning framework for sequential feature extraction and classification with rs-fMRI data, including three parts: (a) dynamic functional connection network construction, (b) temporal features and sequential features extraction, and (c) classification.

Thus, these studies ignore the dynamic characteristics of brain networks. Recent studies have shown that functional connectivity exhibits significant dynamic changes [12,13]. Therefore, many studies focus on analyzing dynamic FC networks, and have a deeper understanding of the basic characteristics of the brain network [14] and dysfunction [15]. Recently, deep learning methods have been applied to the analysis and classification of dynamic FC networks. For example, constitutional neural network-based methods [16,17] have been applied to brain disease diagnosis, and achieve good performance compared to traditional machine learning methods. However, sequence information of temporal features from dynamic FC networks is usually ignored in these studies.

To this end, in this paper, we propose a recurrent neural network (RNN) based learning framework to extract sequential features from dynamic FC networks with rs-fMRI data for AD-related brain disease classification. Figure 1 illustrates the proposed RNN framework for sequential feature extraction and classification with rs-fMRI data, including three parts: (a) dynamic functional connection network construction, (b) temporal features and sequential features extraction, and (c) classification. Specifically, we first divide rs-fMRI time series into multiple overlapping segments using a fixed-size sliding window. For each time series segment, an FC network was constructed by calculating the Pearson's correlation coefficient of blood oxygen level dependent (BOLD) signals from paired brain regions. Then, each FC network is expanded into a row vector and then spliced into a matrix. Then, we construct three convolutional layers to extract high-level features from low-level functional connectivity, and we use the long short-term memory (LSTM) layer to capture long-term temporal dynamics. Finally, two fully connected layers and a softmax layer are used to classify brain diseases. We evaluate the proposed method on 174 subjects with 563 rs-fMRI scans from the Alzheimer's Disease Neuroimaging Initiative (ADNI) database.[1]

[1] http://adni.loni.usc.edu.

Table 1. Characteristics of the studied subjects (Mean ± Standard Deviation). MMSE: Mini-Mental State Examination.

Group	AD	lMCI	eMCI	NC
Male/Female	16/15	27/18	20/30	20/28
Age	74.7 ± 7.4	72.3 ± 8.1	72.4 ± 7.1	76.0 ± 6.8
MMSE	21.8 ± 3.3	27.1 ± 2.1	28.1 ± 1.6	28.8 ± 1.4

The experimental results demonstrate that our proposed method helps improve diagnostic performance.

2 Method

2.1 Subjects and Data Preprocessing

The rs-fMRI data obtained from the ADNI database were studied. We use rs-fMRI data from 174 subjects, including 31 AD, 45 late MCI (lMCI), 50 early MCI (eMCI), and 48 normal controls (NCs). It is worth noting that one subject may have one or more scans at intervals of 6 months to 1 year. There include 99, 145, 165, 154 scans for AD, lMCI, eMCI and NC subject groups, respectively. The specifications of the data acquired for each scan are as follows: the in-plane image resolution is 2.29–3.31 mm, the slice thickness is 3.31 mm, TE (echo time) = 30 ms, TR (repetition time) = 2.2–3.1 s, and there are 140 volumes (time points) for each subject. The demographic and clinical information of these subjects is summarized in Table 1.

The rs-fMRI data are preprocessed using a standard pipeline in the FSL FEAT software package: (1) removal of the first 3 rs-fMRI volumes, (2) slice timing correction, (3) head motion correction, (4) bandpass filtering and (5) regression of white matter, cerebrospinal fluid, and motion parameters. Using the AAL atlas [18] and a deformable registration method [19], the brain space of fMRI scans for each subject is partitioned into 116 regions-of-interest (ROIs). For each ROI, the average rs-fMRI time series is calculated from BOLD signals in all voxels within specific ROIs, which is used as the input for our method.

2.2 Proposed RNN-Based Learning Framework

As shown in Fig. 1, our framework consists of three parts: (a) dynamic functional connection network construction, (b) temporal features and sequential features extraction, and (c) classification. More details can be found below.

Dynamic FC Network Construction. As shown in Fig. 1 (a), with the mean time series of ROIs, we constructed a dynamic FC network based on continuous and overlapping time windows. For each subject, we first segment all rs-fMRI time series into T continuous and overlapping time windows with the constant length L. Then, an FC network (corresponding to an adjacency matrix)

$\mathbf{M}^t \in \mathbb{R}^{N\times N}(t = 1, \cdots, T)$ is constructed by calculating Pearson's correlation coefficient between BOLD signals of paired ROIs at the t-th time window as:

$$\mathbf{M}^t(i,j) = \frac{covar(x_i^t, x_j^t)}{\sigma_{x_i^t}\sigma_{x_j^t}} \tag{1}$$

where *covar* represents the covariance between two vectors, and $\sigma_{x_i^t}$ represents the standard deviation of the vector x_i^t. Here, x_i^t and x_j^t represent the BOLD signal segments of the i-th and j-th ROI in the t-th time window, respectively.

According to the definition in Eq. (1), $\mathbf{M}^t(i,j)$ is used to measure the FC between a pair of brain regions. Therefore, given T time windows/segments, we can generate a set of FC networks $\mathcal{M} = \{\mathbf{M}^1, \mathbf{M}^2, \cdots, \mathbf{M}^T\} \in \mathbb{R}^{T\times N\times N}$ to deliver rich dynamic characteristics of brain FC networks.

Temporal Features and Sequential Features Extraction. Based on the dynamic FC network, we employ three convolutional layers to further extract higher-level brain network features, as shown in Fig. 1 (b). Specifically, we first expand the FC network of each time window into a vector of $1 \times N^2$, so the dynamic FC network is transformed into a matrix $\mathcal{G} \in \mathbb{R}^{T\times N^2}$. For each subject, the matrix $\mathcal{G}$ of T time windows is used as the input of the proposed network. Then, we set up three convolutional layers, and set the size of the three-layer convolution kernel to $S_1 \times N$, $S_2 \times N$ and $S_3 \times 1$, and set the stride of each layer along the time dimension and the space dimension to $(1, N)$, $(1, 1)$ and $(2, 1)$, respectively. Each convolutional layer is followed by batch normalization, rectified linear unit (ReLU) activation, and 0.25 dropout.

For temporal and sequential feature extraction, the convolution along the spatial dimension is the feature mapping for each ROI, which can be understood as calculating a single output value for each ROI by calculating the weighted combination of the functional connectivity between each ROI and all ROIs. This is expected to reflect *spatial changes* centered at each specific ROI. The convolution along the time dimension corresponds to different feature mappings of the same ROI, which can be understood as calculating a single output value for each specific ROI by calculating the weighted combination of the functional connectivity between the same ROI and all ROIs in adjacent time windows. This is expected to reflect *temporal changes* of each specific ROI. It should be emphasized that after each layer of convolution operation, higher-level network dynamic characteristics will be obtained. Therefore, given K_1, K_2 and K_3 channels for these three convolutions, we will get a $T_1 \times N \times K_1$ tensor, a $T_2 \times 1 \times K_2$ tensor and a $T_3 \times 1 \times K_3$ tensor in turn.

To capture the interaction between consecutive adjacent time segments, we use recurrent networks to simulate the temporal dynamic pattern of brain activity. Specifically, we first convert the high-level brain network features learned in the previous layer into an ordered sequence, which will then be handed over to the recurrent network for processing. We use the long short-term memory (LSTM) network to capture the time series patterns and dig deeper into the different contributions between the time series. The LSTM architecture used in

this study is shown in Fig. 1 (b), including an LSTM layer. In this way, the error signal can easily propagate to the bottom layer of the LSTM, thereby reducing the disappearance of the gradient. The LSTM layer (containing 64 neurons) is a representation of the overall functional characteristics and is used to learn time dynamics along the time step.

Classification. As shown in Fig. 1 (c), with the output of LSTM as input, we employ two fully connected layers and a softmax layer for prediction. The first fully connected layer contains 32 neurons. The second fully connected layer contains 16 neurons. There are 2 and 4 neurons in the last fully connected layer for binary and four-category classification, respectively.

Implementation. For the proposed network shown in Fig. 1, we empirically set the parameters as follows: $N = 116, L = 70, T = 34, T_1 = 33, T_2 = 32, T_3 = 13$, $S_1 = 2, S_2 = 2, S_3 = 8, K_1 = 8, K_2 = 16$ and $K_3 = 32$. The Adam optimizer with recommended parameters is used for training, and the number of epochs and batch size are empirically set as 200 and 16, respectively.

3 Experiment

3.1 Experimental Setting

In this study, we employed a 5-fold *subject-level* cross-validation (CV) strategy to ensure that there is no overlap between training and test data. Both binary and multi-class classification experiments are performed, including 1) eMCI vs. NC classification, 2) AD vs. NC classification, and 3) AD vs. lMCI vs. eMCI vs. NC classification. Specifically, for each classification task, all subjects are partitioned into 5 subsets (the size of each subset is roughly the same). Each subset is sequentially selected as the test set, while the remaining four subsets are combined to construct the training set. We further select 20% of the training subjects as validation data to determine the optimal parameters of the model. It is worth noting that, to enhance the model's generalization ability, each scan of each subject is treated as an independent sample, but all scans of the same subject have the same class label. We evaluate the performance by calculating the overall accuracy of all categories and the accuracy of each category.

We compare our method with the following four methods. 1) **Baseline**: In this method, a stationary FC network is first constructed for each subject by computing the Pearson correlation coefficient between the time series of any pair of ROIs. Then, the connectivity strengths of stationary FC networks are used as features. A t-test method with a threshold (*i.e.*, p-value < 0.05) is used for feature selection, followed by a linear SVM with default parameters for classification. 2) **SVM**: In this method, a stationary FC network is first constructed for each subject. Then, local clustering coefficients of the stationary FC network are extracted as features, where t-test and a linear SVM with default parameters are also used for feature selection and classification, respectively. 3) **DFCN-mean** [20]: In this method, a dynamic FC network is first constructed for each subject. Then, the

Table 2. Performance of five methods in two binary classification tasks, *i.e.*, eMCI vs. NC and AD vs. NC classifications. ACC = Accuracy.

Method	eMCI vs. NC (%)			AD vs. NC (%)		
	ACC	ACC_{NC}	ACC_{eMCI}	ACC	ACC_{NC}	ACC_{AD}
Baseline	57.1	48.1	65.6	73.3	77.8	66.7
SVM	63.6	50.0	75.0	75.0	80.0	66.7
DFCN-mean	67.7	47.3	84.7	76.4	**100.0**	33.3
CNN	76.2	77.3	75.2	87.8	92.0	80.0
Proposed	**84.5**	**84.0**	**84.8**	**92.8**	96.7	**86.7**

Table 3. Performance of five methods in the multi-class classification task, *i.e.*, AD vs. lMCI vs. eMCI vs. NC classification. ACC = Accuracy.

Method	AD vs. lMCI vs. eMCI vs. NC (%)				
	ACC	ACC_{NC}	ACC_{eMCI}	ACC_{lMCI}	ACC_{AD}
Baseline	30.6	20.0	38.9	30.0	33.3
SVM	35.0	22.0	69.5	21.0	6.7
DFCN-mean	44.0	36.0	**87.6**	22.0	0.0
CNN	52.8	44.7	47.6	**65.0**	40.0
Proposed	**61.7**	**57.3**	57.1	56.0	**46.7**

temporal and spatial mean features of dFC network are extracted. The manifold regularized multi-task feature learning (M^2TFL) and multi-kernel SVM are used for feature selection and classification [21], respectively. 4) **CNN**: As a variant of our method, this method has a similar network architecture, but is implemented without considering the temporal dynamics along with time steps. That is, we replace the LSTM layer in our method with an average pooling layer.

3.2 Classification Performance

The quantitative results achieved by different methods in two binary and one multi-class classification tasks are reported in Table 2 and Table 3, respectively. As can be seen from Table 2 and Table 3, our proposed method outperforms the competing methods most cases. For instance, our proposed method yields the accuracy of 84.5% and 92.8% for eMCI vs. NC classification and AD vs. NC classification, respectively, while the best accuracies obtained by the competing methods are 76.2% and 87.8%, respectively. For the challenging AD vs. lMCI vs. eMCI vs. NC classification task, our proposed method achieves the overall best accuracy of 61.7%, while the second-best overall accuracy of four competing methods is 52.8%. These results suggest the effectiveness of our proposed method in rs-fMRI based brain disease classification.

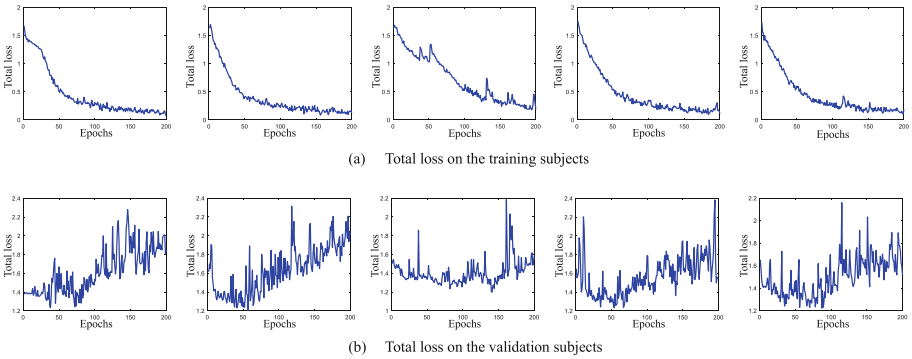

Fig. 2. Total loss of the proposed method with 200 epochs in each fold cross-validation (from left to right) for AD vs. lMCI vs. eMCI vs. NC classification task. Here, (a) total loss on training data, and (b) total loss on validation data.

From Table 2 and Table 3, one can also have more interesting observations. *First*, CNN-based methods (*i.e.*, CNN and our proposed method) generally outperform traditional learning methods (*i.e.*, Baseline, SVM and DFCN-mean). This suggests that CNN can capture the underlying properties of brain networks, and thus can be applied to various tasks of brain network analysis. *Second*, compared with the CNN method, the proposed method can achieve higher performance, which proves the advantage of exploring the temporal information from functional connectivity networks. *Finally*, compared with stationary FC network-based methods (*i.e.*, Baseline and SVM), dynamic FC network-based methods (*i.e.*, DFCN-mean, CNN and our method) can achieve better accuracies, indicating that the dynamics of FC networks can provide useful information for better understanding the pathology of brain diseases.

On the other hand, Fig. 2 presents the total loss on the training subjects and validation subjects in each fold of cross-validation for AD vs. lMCI vs. eMCI vs. NC classification. From Fig. 2, our method can converge fast within 80 epochs.

3.3 Visual Illustration of Discriminative Functional Connectivity

We further conduct an experiment to identify the discriminative brain regions that contribute the most to the specific classification task, and identify the important connectivity between discriminative brain regions.

Specifically, in the brain network high-level feature extraction layer, the output of the first convolutional layer denotes the feature vector of each subject in the T_1 time segments. Since there are $K_1 = 8$ channels in the first convolutional layer, we can construct $K_1 = 8$ feature vectors for each subject, with each feature vector corresponding to a specific channel. For simplicity, we average the feature vectors of all time periods for each channel. Then, using the standard t-test, we measure the group difference of eMCI vs. NC and AD vs. NC, respectively. It is worth noting that, since the obtained feature vectors are different in each fold

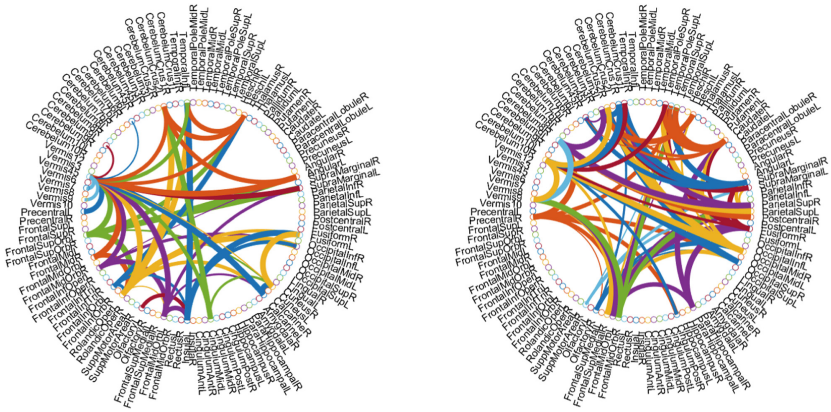

(a) eMCI vs. NC group (b) AD vs. NC group

Fig. 3. Discriminative features for (a) eMCI vs. NC and (b) AD vs. NC classification. Each arc shows the selected feature between two ROIs, where colors are randomly allocated for a better visualization, and the thickness of each arc indicates its discriminative power that is inversely proportional to the corresponding p-value in t-test.

of cross-validation, for each channel, we use the standard t-test for each fold cross-validation, integrating all brain regions with p-values less than 0.05 in the 5-fold cross-validation, and selecting brain regions with 3 or more occurrences as the discriminative brain regions. We further perform the standard t-test on functional connectivity of discriminative brain regions to obtain discriminative features. Figure 3 reports the most discriminative features on the 5th and 7th channels for (a) eMCI vs. NC group and (b) AD vs. NC group, respectively.

As shown in Fig. 3, for eMCI vs. NC classification, the discriminative brain regions we selected include the left fusiform gyrus, the left lobule VI of cerebellar hemisphere, and lobule VII vermis, which are consistent with previous studies [22,23]. For AD vs. NC classification, there are two discriminative brain regions selected by our method, including the left crus I of cerebellar hemisphere and the right lobule IV, V of cerebellar hemisphere. According to previous studies [24], these two brain regions may be biologically associated with AD. These results further validate that our method is potentially helpful in discovering fMRI biomarkers for MCI and AD identification.

4 Conclusion

In this paper, we propose an RNN-based learning framework for AD-related brain disease classification using rs-fMRI time series data. Specifically, a dynamic functional connectivity network is constructed by calculating the correlation between paired brain regions. Then we use three convolutional layers to extract temporal features from dynamic FC networks. After that, we further employ

the LSTM to capture the sequential information of temporal features along with multiple time segments, and employ two fully connected layers for classification. Experimental results on 174 subjects with rs-fMRI data from the ADNI dataset demonstrate the effectiveness of our proposed method.

Acknowledgment. K. Lin, B. Jie, P. Dong, X. Ding and W. Bian were supported in part by NSFC (Nos. 61976006, 61573023, 61902003), Anhui-NSFC (Nos. 1708085MF145, 1808085MF171) and AHNU-FOYHE (No. gxyqZD2017010).

References

1. Fan, L., et al.: New insights into the pathogenesis of Alzheimer's disease. Front. Neurol. **10**, 1312 (2020)
2. Reiman, E.M., Langbaum, J.B., Tariot, P.N.: Alzheimer's prevention initiative: a proposal to evaluate presymptomatic treatments as quickly as possible. Biomark. Med. **4**(1), 3–14 (2010). PMID: 20383319
3. Liu, M., Zhang, J., Adeli, E., Shen, D.: Landmark-based deep multi-instance learning for brain disease diagnosis. Med. Image Anal. **43**, 157–168 (2018)
4. Zhang, L., Wang, M., Liu, M., Zhang, D.: A survey on deep learning for neuroimaging-based brain disorder analysis. Front. Neurosci. **14** (2020)
5. Lee, M., Smyser, C., Shimony, J.: Resting-state fMRI: a review of methods and clinical applications. Am. J. Neuroradiol. **34**(10), 1866–1872 (2013)
6. Jie, B., Zhang, D., Gao, W., Wang, Q., Wee, C.Y., Shen, D.: Integration of network topological and connectivity properties for neuroimaging classification. IEEE Trans. Biomed. Eng. **61**(2), 576–589 (2014)
7. Shen, H., Wang, L., Liu, Y., Hu, D.: Discriminative analysis of resting-state functional connectivity patterns of schizophrenia using low dimensional embedding of fMRI. NeuroImage **49**(4), 3110–3121 (2010)
8. Jie, B., Liu, M., Zhang, D., Shen, D.: Sub-network kernels for measuring similarity of brain connectivity networks in disease diagnosis. IEEE Trans. Image Process. **27**(5), 2340–2353 (2018)
9. Wang, M., Lian, C., Yao, D., Zhang, D., Liu, M., Shen, D.: Spatial-temporal dependency modeling and network hub detection for functional MRI analysis via convolutional-recurrent network. IEEE Trans. Biomed. Eng. **67**(8), 2241–2252 (2020)
10. Wang, M., Zhang, D., Huang, J., Yap, P.T., Shen, D., Liu, M.: Identifying autism spectrum disorder with multi-site fMRI via low-rank domain adaptation. IEEE Trans. Med. Imaging **39**(3), 644–655 (2019)
11. Sporns, O.: The human connectome: a complex network. Ann. N. Y. Acad. Sci. **1224**(1), 109–125 (2011)
12. Hutchison, R.M., et al.: Dynamic functional connectivity: promise, issues, and interpretations. NeuroImage **80**, 360–378 (2013)
13. Zhang, J., et al.: Neural, electrophysiological and anatomical basis of brain-network variability and its characteristic changes in mental disorders. Brain **139**(8), 2307–2321 (2016)
14. Kudela, M., Harezlak, J., Lindquist, M.A.: Assessing uncertainty in dynamic functional connectivity. NeuroImage **149**, 165–177 (2017)
15. Damaraju, E., et al.: Dynamic functional connectivity analysis reveals transient states of dysconnectivity in schizophrenia. NeuroImage: Clin. **5**, 298–308 (2014)

16. Jie, B., Liu, M., Lian, C., Shi, F., Shen, D.: Designing weighted correlation kernels in convolutional neural networks for functional connectivity based brain disease diagnosis. Med. Image Anal. **63**, 1–14 (2020)
17. Kawahara, J., et al.: BrainNetCNN: Convolutional neural networks for brain networks. Towards predicting neurodevelopment. NeuroImage **146**, 1038–1049 (2016)
18. Tzourio-Mazoyer, N., et al.: Automated anatomical labeling of activations in SPM using a macroscopic anatomical parcellation of the MNI MRI single-subject brain. NeuroImage **15**(1), 273–289 (2002)
19. Vercauteren, T., Pennec, X., Perchant, A., Ayache, N.: Diffeomorphic demons: efficient non-parametric image registration. NeuroImage **45**(1), S61–S72 (2009)
20. Jie, B., Liu, M., Shen, D.: Integration of temporal and spatial properties of dynamic connectivity networks for automatic diagnosis of brain disease. Med. Image Anal. **47**, 81–94 (2018)
21. Zhang, D., Shen, D.: Multi-modal multi-task learning for joint prediction of multiple regression and classification variables in Alzheimer's disease. NeuroImage **59**(2), 895–907 (2012)
22. Bokde, A.L.W., et al.: Functional connectivity of the fusiform gyrus during a face-matching task in subjects with mild cognitive impairment. Brain **129**(5), 1113–1124 (2006)
23. Thomann, P.A., Schläfer, C., Seidl, U., Santos, V.D., Essig, M., Schröder, J.: The cerebellum in mild cognitive impairment and Alzheimer's disease - a structural MRI study. J. Psychiatr. Res. **42**(14), 1198–1202 (2008)
24. Suk, H.I., Wee, C.Y., Lee, S.W., Shen, D.: Supervised discriminative group sparse representation for mild cognitive impairment diagnosis. Neuroinformatics **13**, 277–295 (2015)